ARCHIVES OF ELECTRICAL ENGINEERING VOL. 71(3), pp. 627–639 (2022)

DOI 10.24425/aee.2022.141675

Novel optimization method for mobile magnetostatic shield and test applications

PATRICK ALEXANDER RALF ✉, CHRISTIAN KREISCHER

Helmut Schmidt University, University of the Federal Armed Forced Hamburg
Germany
e-mail: {✉ralfp//christian.kreischer}@hsu-hh.de

(Received: 14.12.2021, revised: 31.03.2022)

Abstract: This article provides an optimized solution to the problem of passive shielding against static magnetic fields with any number of spherical shells. It is known, that the shielding factor of a layered structure increases in contrast to a single shell with the same overall thickness. For the reduction of weight and cost by given material parameters and available space the best system for the layer positions has to be found. Because classic magnetically shielded rooms are very heavy, this system will be used to develop a transportable Zero-Gauss-Chamber. To handle this problem, a new way was developed, in which for the first time the solution with regard to shielding and weight was optimized. Therefore, a solution for the most general case of spherical shells was chosen with an adapted boundary condition. This solution was expanded to an arbitrary number of layers and permeabilities. With this analytic solution a differential evolution algorithm is able to find the best partition of the shells. These optimized solutions are verified by numerical solutions made by the Finite Element Method (FEM). After that the solutions of different raw data are determined and investigated.

Key words: differential evolution, evolutionary algorithm, magnetostatic passive shielding, mobile application, optimization, spherical shells

1. Introduction

The shielding against electromagnetic fields is in many domains of industry and science vitally important. A special challenge is represented by the static magnetic fields, because they permeate matter more or less unhindered. There are only three ways to shield against magnetostatic fields, which are the Meissner effect of superconductivity, active shielding with counter-fields or refraction by high permeable material. In this paper, only the shielding with high permeable materials

will be treated. This type of shielding is necessary in different technical applications and scientific experiments. For an application-oriented example, there are a lot of manufactured parts which have to be free of magnetism to a certain degree. This could be tools during precise manufacturing processes [11], parts with high requirements like rolling elements, injectors, or gear drives in the automobile industry [12] as well as measuring equipment like the magnaflux test [1]. These parts can be measured in nearly field-free environments only. In some research areas, for example, electron microscopy, magnetometry or in ultracold atomic physics, nonmagnetic components are mandatory in experiments [2]. The demand for degaussing technology is projected to grow in the next years by about several percent [3]. Therefore, particularly in an industrial environment, a need for local measurements at the customer exists as a unique feature. The common magnetic shielding rooms (MSRs) with very high shielding factors are large and heavy, and that is why they are stationary and fixed in buildings. To make an equivalent MSR transportable, the weight has to be minimized. For this reason, the phenomena of multi-lamellar shells [4] in an optimal arrangement of layers is used. Therefore, a modified, known way to describe the shielding factor analytically is generated and is used further to optimize this solution with respect to shielding performance and weight by a differential evolution algorithm. Because there are no direct comparable findings in the recent literature, it is important to advance this problem statement. Besides the analytical solution, different works treat this problem approximately. In 1916, Ernest Wilson and John William Nicholson introduced a solution by recurrence formulae [13]. Louis V. King generated a solution for thin shells at low frequencies in 1933 [14]. The solution by Wilson and Nicholson was improved by Felix Schweizer in 1961, and his error was corrected by Y.Y. Reutov in 2001 [15]. The optimization by the FEM was made in 2019 for a multilayered cylindrical system [2].

2. Analytical foundations

An analytical way to calculate the magnetic field with permeable material inside the solution space is always by solving proper Maxwell's equations. In the magnetostatic case these equations are

$$\vec{\nabla} \cdot \vec{H} = 0, \tag{1}$$

$$\vec{\nabla} \times \vec{H} = \vec{j}. \tag{2}$$

In Eqs. (1) and (2) $\vec{H}$ is the magnetic field strength and $\vec{j}$ is the current density. Because the external magnetic field shall be given as a source in the boundary conditions, there are no currents inside the solution space, and therefore, the current density is zero: $\vec{j} = \vec{0}$. Further, a magnetic scalar potential of the form $-\vec{\nabla}\psi = \vec{H}$ can be defined [7]. If this scalar potential is inserted into Eq. (1) a Laplace equation arises as:

$$\vec{\nabla}^2 \psi = 0. \tag{3}$$

Equation (2) is automatically fulfilled. A solution for the potential ψ is necessary to use an evolutionary algorithm for finding the best parameters of the shielding geometry. In this case, these solutions have to describe the shielding factor S for multi-lamellar centric spheres against

the outer static magnetic field H_0, which is defined as the relation between the external to the innermost field H_{shield}:

$$S = \frac{H_0}{H_{\text{shield}}}\,. \tag{4}$$

Spherical shells were chosen because they represent the most general case and an analytical solution exists [5]. The shielding problem of a single hollow sphere with a magnetic source inside has been solved by James Clerk Maxwell [6] and it has been expanded to an infinite amount of shells by Arthur William Rücker [4]. A solution for a hollow sphere inside an infinite magnetic field was found by John Davin Jackson [7]. To get the suitable solution, the way of A.W. Rücker will be combined with the boundary conditions of J.D. Jackson.

2.1. Combined solution of J.C. Maxwell and J.D. Jackson

The following equations are expressed in the International System of Units and solved according to today's standards. The final solution is based upon the solution of the Laplace equation of the scalar potential ψ by J.C. Maxwell for a hollow sphere. To solve the Laplace equation for spherical problems, it is often necessary to use spherical coordinates (Fig. 2). To solve this equation, a mathematical approach with the separation of variables is made in the following form:

$$\psi(ru\varphi) = R(r)U(u)\Phi(\varphi). \tag{5}$$

In Eq. (5) r is the radial component, φ is the azimuthal component and u represents the polar component, as well as R, Φ and U are the dedicated functions. The usual notation θ for the polar component was replaced by the substitution $u = \cos\theta$ to simplify the basic equation. By converting the Laplace equation, the equation can be separated into a system of three ordinary differential equations (ODEs):

$$\frac{\mathrm{d}}{\mathrm{d}x}\left(r^2\frac{\mathrm{d}R}{\mathrm{d}r}\right) = l(l+1)R, \tag{6}$$

$$\frac{\mathrm{d}^2\Phi}{\mathrm{d}\varphi^2} + \Phi m^2 = 0, \tag{7}$$

$$\frac{1-u^2}{U}\frac{\mathrm{d}}{\mathrm{d}u}\left((1-u^2)\frac{\mathrm{d}U}{\mathrm{d}u}\right) = m^2 - l(l+1)(1-u^2). \tag{8}$$

For lack of space, the input arguments are omitted. The constants l and m appear during the separation and they are chosen in such a way, that it is easier to solve the equations later. The solutions of these ODEs are generated by the power approach $R = r^{\lambda}$, an exponential ansatz $\Phi = e^{\lambda\varphi}$ and by a power series method for U [9]. The solutions are

$$R_l(r) = A_l r^l + B_l r^{-l-1}, \tag{9}$$

$$\Phi_m(\varphi) = A_m \exp(\mathrm{i}m\varphi) + B_m \exp(-\mathrm{i}m\varphi)\,, \tag{10}$$

$$U_{lm}(u) = (-1)^m\left(1-u^2\right)^{\frac{m}{2}}\frac{1}{2^l l!}\frac{\mathrm{d}^{l+m}}{\mathrm{d}u^{l+m}}\left(u^2-1\right)^l. \tag{11}$$

In these solutions A_{lm} and B_{lm} are constants. Equation (10) can be transformed to

$$\Phi_m(\varphi) = K_m \exp(\mathrm{i}m\varphi),$$

with

$$K_m = \sqrt{(C_m \cos(m\varphi))^2 + (D_m \sin(m\varphi))^2},$$
$$C_m = A_m + B_m \quad \text{and} \quad D_m = A_m - B_m .$$

If the angular dependent equations are scaled, then Eqs. (9) to (11) are inserted into the separation approach (Eq. (5)), the following solution for the potential is generated:

$$\psi(ru\varphi) = \left(A_{lm} r^l + \frac{B_{lm}}{r^{l+1}}\right) e^{\mathrm{i}m\varphi} \frac{1}{\sqrt{2\pi}} N_{lm} U_{lm}(u). \tag{12}$$

Here is $A_{lm} = \dfrac{A_l}{K_m}$ and $B_{lm} = \dfrac{B_l}{K_m}$ as well as the scaling factor

$$N_{lm} = \sqrt{\frac{(l-m)!}{(l+m)!}\frac{2l+1}{2}} .$$

With the definition of the spherical harmonics Y_{lm} [10], the Rodrigues formula and after the inverse substitution of u, it follows that:

$$\psi(r\theta\varphi) = \left(A_{lm} r^l + \frac{B_{lm}}{r^{l+1}}\right) Y_{lm}(\theta, \varphi). \tag{13}$$

This solution only depends on the control variables l and m. Because the geometry as well as the arising field are radial symmetric to the axis in the direction of the field $\vec{H}_0$, the control variable m can be set to zero ($m = 0$) [10]. This means the solution does not depend on the angle φ, whereby the imaginary term disappears and the spherical harmonics Y become real, they are called now surface harmonics S:

$$\mathsf{S}_l(\theta) = \sqrt{\frac{2l+1}{4\pi}} P_l(\cos\theta). \tag{14}$$

In Eq. (14), P_l represents the Legendre polynomials, which are generated from the spherical harmonics for $m = 0$. The general solution is, therefore:

$$\psi(r\theta) = \sum_l C_l r^l \mathsf{S}_l(\theta), \tag{15}$$

where $l \in \mathbb{Z}$. For this solution of the Laplace equation, a distinction of cases has to be made, because there are three different areas for a hollow sphere. In the inner area, the constant C_l for all negative powers of r has to be zero to avoid singularities for $r = 0$. Inside the shell there are no restrictions concerning the constants.

In the outer area, C_l has to be zero for all positive powers of r, because the magnetic field cannot become an infinite magnitude. If the solution is changed by the boundary conditions of

J.D. Jackson, there are three different solutions for each solution space ((16) – inside, (17) – shell, (18) – outside):

$$\psi_i(r\theta) = \sum_l \alpha_l r^l \mathsf{S}_l(\theta), \tag{16}$$

$$\psi_m(r\theta) = \sum_l \left(\beta_l r^l + \frac{\gamma_l}{r^{l+1}}\right) \mathsf{S}_l(\theta), \tag{17}$$

$$\psi_a(r,\theta) = H_0 r\cos\theta + \sum_l \frac{\delta_l}{r^{l+1}} \mathsf{S}_l(\theta). \tag{18}$$

In Eqs. (16) to (18) α, β, γ and δ are the coefficients of the general solution.

2.2. Solution of A.W. Rücker

For the case of an arbitrary number of layers, the boundary conditions for each layer has to be defined. They are necessary to get the coefficients of the equations above. These can be found by the interface conditions between the surfaces of the layers (see Fig. 1). Currently, the sums in Eqs. (16) up to (18) are not restricted. The crucial summand is the one with $l = 1$ [4,7]. For every interface of the layers there are two conditions, both for the normal part of the field $\vec{H}_n$ as well as the tangential part of the field $\vec{H}_t$. For the magnetic field they are

$$\mu_1 \vec{H}_{1n} = \mu_2 \vec{H}_{2n}\,, \tag{19}$$

$$\vec{H}_{1t} = \vec{H}_{2t}\,. \tag{20}$$

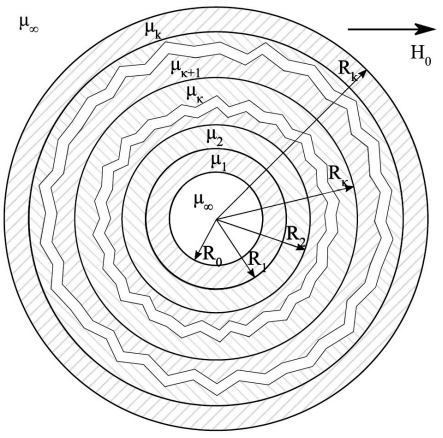

Fig. 1. A cross section of k layers for the mathematical model

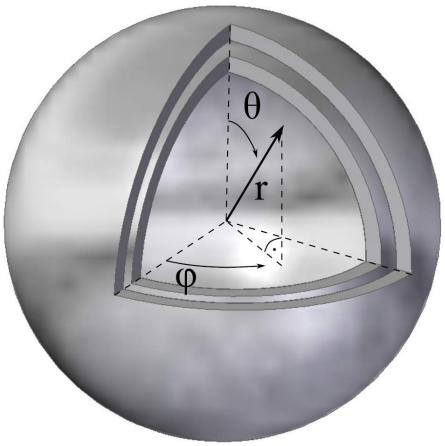

Fig. 2. The spherical coordinates of a three layer model for example

Respectively, with the definition of the scalar potential, where the indices are $n = r$ and $t = \theta$

$$\frac{\partial \psi_1}{\partial r} = \frac{\mu_2}{\mu_1}\frac{\partial \psi_2}{\partial r}\,, \tag{21}$$

$$\frac{\partial \psi_1}{\partial \theta} = \frac{\partial \psi_2}{\partial \theta} \,. \tag{22}$$

Together with Eqs. (16) to (18) a linear system of equations can be generated (see Eqs. (23) to (28)) for the transition from the inner area to the first shell, between the layers and from the last shell to the outer area:

$$\mu_\infty R_0^3 \alpha - \mu_1 R_0^3 \beta_1 + \mu_1 2\gamma_1 = 0, \tag{23}$$

$$-R_0^3 \alpha + R_0^3 \beta_1 + \gamma_1 = 0, \tag{24}$$

$$\mu_\kappa R_\kappa^3 \beta_\kappa - \mu_\kappa 2\gamma_\kappa - \mu_{\kappa+1} R_\kappa^3 \beta_{\kappa+1} + \mu_{\kappa+1} 2\gamma_{\kappa+1} = 0, \tag{25}$$

$$-R_\kappa^3 \beta_\kappa - \gamma_\kappa + R_\kappa^3 \beta_{\kappa+1} + \gamma_{\kappa+1} = 0, \tag{26}$$

$$\mu_k R_k^3 \beta_k - \mu_k 2\gamma_k + \mu_\infty 2\delta = \mu_\infty R_k^3 \frac{1}{C_N} H_0 \,, \tag{27}$$

$$-R_k^3 \beta_k - \gamma_k + \delta = -R_k^3 \frac{1}{C_N} H_0 \,. \tag{28}$$

Because $l = 1$, the sum over l in Eqs. (16) to (18) is eliminated, so that Eqs. (23) to (28) are indicated by the number of shells k with $\kappa \in]\,0 \ldots k\,[$. In these equations the variable μ_∞ is the relative permeability of the inner and outer space, R is the radius of the shells and C_N is a scaling factor from the surface harmonic. In the general solution the polar and the azimuthal terms are scaled to make the input arguments become independent because the general solution is valid for all spherical geometries. With this scaling the surface harmonics become more general spherical harmonics, which are necessary to represent the solution of the Laplace equation. With the radial term and the (scaled) spherical harmonics, every possible solution of the Laplace equation can be generated.

3. Verification by FEM

To prove that the analytical way of describing the problem is correct, some analytical solutions will be compared with numerical solutions made by the FEM using the Ansys Maxwell program. Therefore, the analytical solution is added into a Matlab code, which graphs the magnetic field strength as well as the potential, magnetic induction and streamlines of the field. Further, it calculates the magnitude of the inner field $\left|\vec{H}\right|$ respective to $\left|\vec{B}\right|$. For the comparison, an arbitrary model can be used. To show that the analytical solution works for each number of shells, a few models with a different number of shells will be investigated. For example, a model with two shells (three layers) is shown in Fig. 3.

If the field profile from Fig. 3 is compared with this from Fig. 4, it shows that they are equal to each other. The difference in colors is a result of differently stored color maps of the computer programs. From Table 1 it is apparent that the difference between the solutions is very small. This deviation may be caused by the implied approximation of the FEM and a middle coarse mesh. Because of this result it can be acted on the assumption, that the analytical solution is correct.

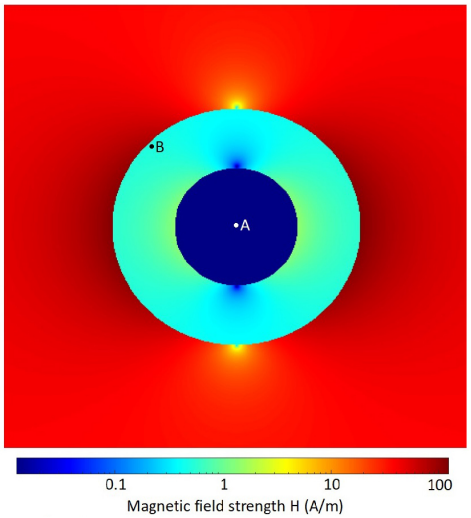

Fig. 3. A cross section in the direction of the field profile. The colors show the magnitude of the magnetic field strength of the analytical solution

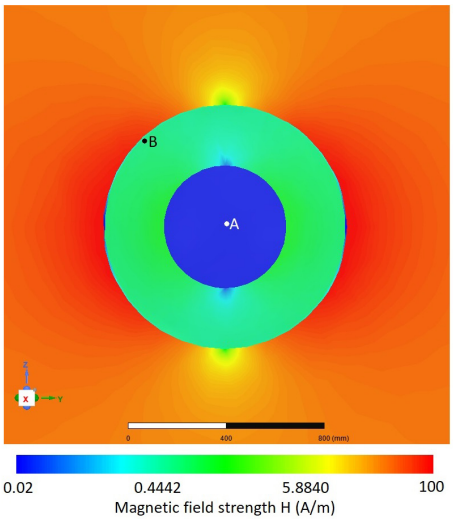

Fig. 4. A cross section in the direction of the field profile. The colors show the magnitude of the magnetic field strength of the numerical solution

Table 1. Comparison of two different positions

Position	**$\|H\|$ Matlab in A/m**	**$\|H\|$ FEM in A/m**	**Deviation in ‰**
A	0.002353	0.002379	1.105
B	0.501	0.5084	1.477

4. Optimization by a differential evolution algorithm

For the global optimization of this problem, the method of differential evolution (DE) is used. This algorithm belongs to the class of evolutional algorithms, whose natural evolution is ideal. That means that there are individuals, which represent a population whose parameters will be changed in every iteration step, which makes a new generation. In this process, an optimum of a defined output value (the best generation) will be found by varying different parameters and continued every time with the best population (see Fig. 5).

The optimal solution is the best individual from the last population. Like in nature, there are different operators, which have an effect on individuals depending on the population. In this case these are: the differential weight F, the crossover probability CR and the mutation probability M [8]. These parameters have a significant effect on the behavior of the algorithm, and therefore, they are shown in Table 2.

The differential weight F defines the percentage of the used differences, which are added to the population during the variation/mutation. These differences are made by both the pop-

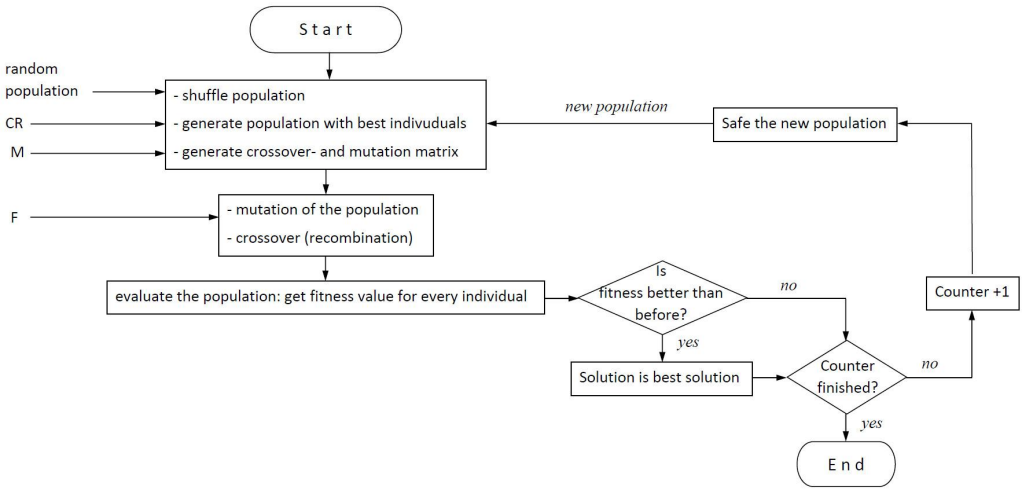

Fig. 5. A flowchart of the main loop of the differential evolutional algorithm

Table 2. Values of the different operators

Parameter	***F***	***CR***	***M***
Value	0.85	0.7	0.5

ulation with only the best members of the actual population (direction of the algorithm) and the shuffled populations (exploration of the solution space). The crossover probability CR defines the random part of the mutated population, which will be recombined. For $CR = 1$, the recombined population is the mutated population and for $CR = 0$ there is no recombination. The mutation probability M defines which random individuals from the old population should be variated/mutated. For $M = 1$, all members of the population will be mutated, and for $M = 0$, no one will be mutated. The values of these parameters, based on the programming code, are constant and were chosen according to the approved values from [8]. The number of populations was set to 100.

In this DE the minimum of this output value is sought after. To start with, a random population is generated, which individuals consist of a vector with the positions of the shells as components. This type of evolutionary algorithm is in principle able to optimize after every existing value. But not all values are meaningful to optimize. If the permeability were some of these values, the algorithm would always find the highest value inside the solution range. Therefore, some definitions have to be made. A common case, where the permeability and thickness of the shells are constant will be used. Furthermore, the air between the shells and the inner- and outermost position of the shells are constant too. The optimization looks for the optimal system of the shells inside. During the procedure, a number of solutions are generated by a fitness function, which assigns a quality value to every individual. With this quality value the best individuals can be localized.

4.1. The fitness function

The fitness function is crucial in which direction the optimization process will be regulated. In this case the fitness function identifies the best positions of the shells. That means the input arguments are the positions and the output variable is the shielding factor for the simplest case. For a given number of shell positions, the best system generates the highest shielding factor. For this purpose, the solved variables from heading 2 are used for the calculation of the magnetic field. The base for the fitness function is the analytical solution. It consists of solving the system of linear equations (see Eqs. (23) to (28)) in heading 2.2. With the solved constants, Eqs. (16) to (18) are complete and the magnetic field can be calculated by differentiation. Because the inner field is homogeneous and do not depend on r (see Eqs. (29) and (30)), the variable $\alpha \cdot C_N$ is a measure for the magnitude of the inner magnetic field.

$$H_{r,i} = \alpha \cdot C_N \cdot \cos\theta, \tag{29}$$

$$H_{\theta,i} = -\alpha \cdot C_N \cdot \sin\theta. \tag{30}$$

Because the algorithm searches for a global minimum, the output value of the fitness function has to be small if an individual is a good solution. Because a good shielding factor S should be very high, the fitness function f has to be adjusted. Further, it shall be optimized in terms of weight. Therefore, the fitness function is expanded with an equation, which calculates the whole volume V of the shells. Because of that, the fitness function has the form:

$$f\left(R_1, R_2, \ldots, R_k\right) = \frac{V\left(R_1, R_2, \ldots, R_k\right)}{S\left(R_1, R_2, \ldots, R_k\right)}. \tag{31}$$

In the last step, unphysical solutions have to be eliminated. It is possible, that there are individuals in the random start population, whose position values are not sorted. This means the position of a larger shell is before a smaller shell. This also can happen due to the mutation of some individuals. Mathematically, the algorithm and fitness function are able to find a solution, but negative shielding factors or voluminal are not physically reasonable. This problem is solved by assigning very high values to these solutions by means of a retrieval loop. At least it has to be verified that the algorithm can find an approximated global optimum. The algorithm has to find the same solution every time and it has to be the right solution. For the first condition, the algorithm will be run 10 times and controlled if the solution does not change. This procedure has shown, that the solution is always the same, it only differs in the 4^{th} decimal place (see Table 3). For this, a model with five shells (9 layers) was used. The inner radius is 0.5 m, the outer radius is 1 m and the permeability is 15 000. This is the permeability of Mu-metal, a common alloy for magnetic shields. It was chosen because a prototype for later experiments will be made of this material.

For the second condition a model with three shells is used, where the position of the middle shell is changed numerically to find the best solution iterative. The reference value, found by the DE, is 0.6709 m. As part of the approximation of the FEM, the optimal solution of the numerical calculation is about 0.668 m. Summarized, it follows that the algorithm works correctly.

Table 3. Positions of the shells

Trial no.	Position 1 in m	Position 2 in m	Position 3 in m
1	0.5731	0.6671	0.7967
2	0.5730	0.6670	0.7967
3	0.5730	0.6670	0.7967
4	0.5730	0.6670	0.7967
5	0.5730	0.6670	0.7967
6	0.5730	0.6670	0.7967
7	0.5731	0.6670	0.7967
8	0.5730	0.6670	0.7967
9	0.5730	0.6670	0.7967
10	0.5731	0.6671	0.7967

4.2. Results for selected cases

In this section, the influence of constant model parameters shall be investigated. For this purpose, the basic model with three shells is used. There are four parameters that can be varied. These are the inner radius R_0, the outer radius R_k, the thickness of the shells lt and the permeability μ. First of all, the thickness and permeability are constant and the radii will be varied. The thickness is set to 0.001 m and the relative permeability is 15 000. The range of the radii goes up to 1 m.

Figure 6 shows that there are only for the nonphysical cases of $R_0 \cong 0$ or $R_0 \cong R_k$ a linear behavior of the graph. For the regular cases there is a nonlinear behavior. That means there is no fixed relation of the optimal position of the middle shell to the position of the inner shell respective to the outer shell. The optimal solution depends directly on the model itself and its parameters.

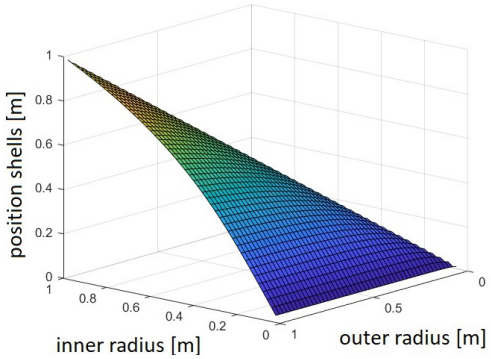

Fig. 6. All optimized solutions for the position of the middle shell in dependence of the inner and outer radii

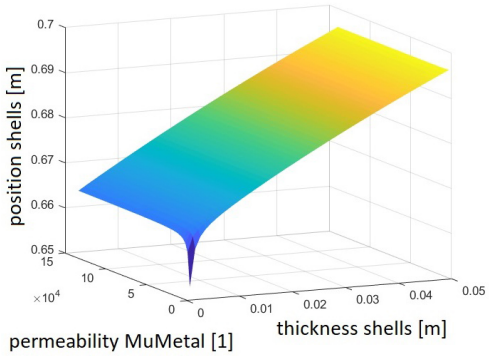

Fig. 7. All optimal solutions for the position of the middle shell in dependence of the thickness and the permeability

The dependence of the thickness and the permeability can be investigated if the radii are constant. The permeability goes from zero to 15 000 and the thickness from zero to 0.05 m. Figure 7 shows, that there is no dependence of the permeability on the solution. All values along the permeability axis are constant. The effect of the thickness of the shells causes a larger radius of the middle shell with an approximately linear behavior. If the permeability or the thickness of the shells goes to zero, there is some kind of singularity (see Fig. 8). At this point, the algorithm is still able to find a solution but it converges to 0.5 m. All things considered the geometry in general has a significant effect on the optimal position of the middle shell. In the case of models with more shells, the same effect of nonlinearity can be observed (see Figs. 9 and 10).

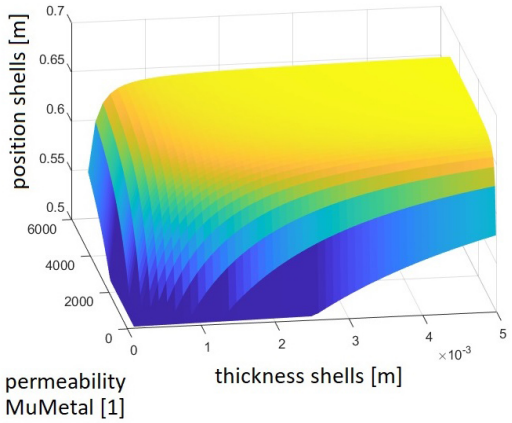

Fig. 8. A closer view of the singularity from Fig. 7

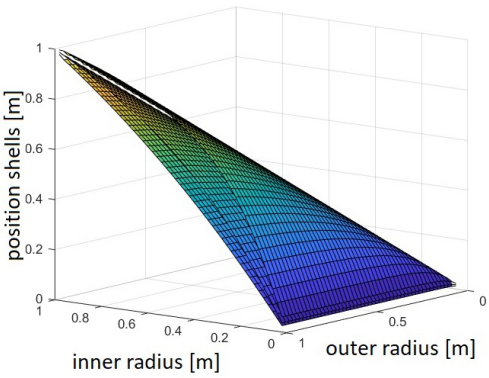

Fig. 9. The optimal positions for a model with 5 shells (9 layers) and constant thickness and permeability

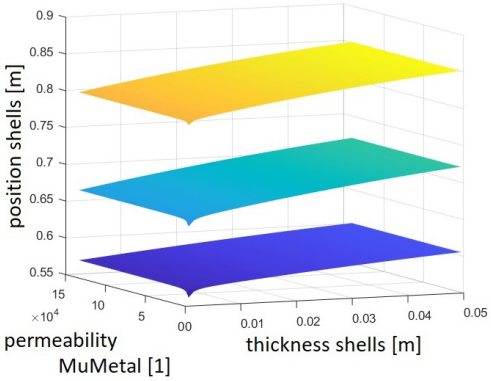

Fig. 10. The optimal positions for a model with 5 shells (9 layers) and constant inner and outer radii

It shows that the effect of the optimized positions of the shells is different. For constant permeability and thickness, the behavior of the position with the smallest radius is more or less

linear, whereas the position with the biggest radius shows a strong nonlinear behavior. In contrast to the case where the radii are constant, each behavior is equal and the relation between the positions is the same.

5. Summary and conclusion

In the first section, it was shown, that the analytical solution for the general case of spherical shielding with the theoretical boundary condition of an infinite external magnetic field is, on the one hand, correct and, on the other hand, sufficiently represents the solution close to the shielding geometry. This is important because the used evolutional algorithm needs a good working fitness function to work accurately. After the adaptation of the analytical solution into the fitness function by generating a correct relation of the command variables and eliminating unphysical solutions, FEM analyses have shown that the differential algorithm works proper.

With this algorithm, different solutions for diverse models were investigated to make fundamental statements about a general optimal system for high permeable shells. The solutions show that the optimal system for the shells depends strongly on the positions, as well as on the thickness of the shells. That means, on the one hand, there is always an optimal solution but, on the other hand, there is no constant relation between systems with the same number of shells. For further investigations and/or constructions, it is now possible to minimize the size and hence the weight as well as the cost for any multi-layered magnetically shielded chambers. It is obvious that for other problems with different geometries such as cylinders or cubes, there are also optimal solutions.

For practical use, it is necessary either to calculate the optimal solution for an individual problem statement every time, or its possible to generate empiric equations for a defined area of applications. In the first procedure the developed Matlab code has to be slightly modified, or a graphic user interface has to be programmed. If the maximum size of the shielding is known, it is easier to store some empiric equations for usual problem statements, that can be used for a fast calculation of a constructional sketch.

Acknowledgment

This work is supported by the Federal Ministry for Economic Affairs and Energy on the basis of a decision by the German Bundestag as part of cooperation project 'Entwicklung einer innovativen Entmagnetisierungseinheit mittels einer neuartigen Sandwichstruktur zur Abschirmung von äußeren magnetischen Störgrößen sowie eines Sensornetzwerks zur echtzeit-Kompensation' in the ZIM program (german: 'Zentrales Innovationsprogramm Mittelstand' which means 'Central Innovation Programme for small and medium-sized enterprises').

Supported by:

Federal Ministry for Economic Affairs and Energy

on the basis of a decision by the German Bundestag

ZIM Zentrales Innovationsprogramm Mittelstand

References

[1] Schiebold K., *Zerstörungsfreie Werkstoffprüfung – Magnetpulverprüfung*, Springer-Verlag (2015).

[2] Farolfi A., Trypogeorgos D., Colzi G., Fava E., Lamporesi G., Ferrari G., *Design and characterization of a compact magnetic shield for ultracold atomic gas experiments*, Review of Scientific Instruments, 90.11, 115114 (2019), DOI: 10.48550/arXiv.1907.06457.

[3] Report Buyer Ltd., *Degaussing System Market by Solution, End User, Vessel Type and Region – Global Forecast to 2023*, June (2018).

[4] Rücker A.W., *VII. On the magnetic shielding of concentric spherical shells*, The London, Edinburgh, and Dublin Philosophical Magazine and Journal of Science, 37.224, pp. 95–130 (1894).

[5] Baum E., Bork J., *Systematic design of magnetic shields*, Journal of Magnetism and Magnetic materials, 101.1-3, pp. 69–74 (1991).

[6] Clerk Maxwell J., *Electricity and magnetism*, vol. 2, New York: Dover (1954).

[7] David Jackson J., *Classical Electrodynamics*, American Association of Physics Teachers (1999).

[8] Karaboğa D., Ökdem S., *A simple and global optimization algorithm for engineering problems: differential evolution algorithm*, Turkish Journal of Electrical Engineering and Computer Sciences, 12.1, pp. 53–60 (2004).

[9] Bronstein I.N., Hromkovic J., Luderer B., Schwarz H.R., Blath J., Schied A., Gottwald S., *Taschenbuch der Mathematik*, compact disc, Springer-Verlag (2008).

[10] Bartelmann M., Feuerbacher B., Krüger T., Lüst D., Rebhan A., Wipf A., *Theoretische Physik 2 |Elektrodynamik*, Springer-Verlag (2018).

[11] Rohner M., *Magnetisch anhaftende Partikel zuverlässig entfernen*, JOT Journal für Oberflächentechnik, 53, pp. 51–53 (2013).

[12] Maurer Magnetic AG, *Restmagnetismus – das verkannte Problem*, JOT Journal für Oberflächentechnik, 57, pp. 104–105 (2017).

[13] Wilson E., Nicholson J.W., *On the magnetic shielding of large spaces and its experimental measurement*, Proceedings of the Royal Society of London, Series A, Containing Papers of a Mathematical and Physical Character, pp. 529–549 (1916).

[14] King L.V., *XXI. Electromagnetic shielding at radio frequencies*, The London, Edinburgh, and Dublin Philosophical Magazine and Journal of Science, 15.97, pp. 201–223 (1933).

[15] Reutov Y.Y., *Choice of the number of shells for a spherical magnetostatic shield*, Russian Journal of Non-destructive Testing, 37.12, pp. 872–878 (2001).